ISSN 1995-0780, Nanotechnologies in Russia, 2017, Vol. 12, Nos. 3–4, pp. 208–217. © Pleiades Publishing, Ltd., 2017.

A Software Package for Computer-Aided Design of Spintronic Nanodevices[1]

A. A. Knizhnik[a,b]*, I. A. Goryachev[a], G. D. Demin[a,c], K. A. Zvezdin[a,f], E. V. Zipunova[a], A. V. Ivanov[a,e], I. M. Iskandarova[a,b], V. D. Levchenko[a,e], A. F. Popkov[a,c,d], S. V. Solov'ev[a,c], and B. V. Potapkin[a,b]

[a]*Kintech Lab. Ltd., Moscow, 123182 Russia*

[b]*NRC "Kurchatov Institute," Moscow, 123182 Russia*

[c]*National Research University of Electronic Technology, Zelenograd, 124498 Russia*

[d]*Moscow Institute of Physics and Technology (State University), Dolgoprudny, Moscow oblast, 141701 Russia*

[e]*Keldysh Institute of Applied Mathematics, Russian Academy of Sciences, Moscow, 125047 Russia*

[f]*Prokhorov General Physics Institute, Russian Academy of Sciences, Moscow, 119991 Russia*

**e-mail: knizhnik@kintechlab.com*

Received September 30, 2016; in final form, December 13, 2016

Abstract—Spintronics is a new trend in the development of nanoelectronics and, therefore, requires the development of new software tools for modeling aimed at the development and further miniaturization of spintronic devices. In this paper, we present a new software package for the technology computer aided design modeling of spintronic devices based on magnetic tunnel junctions. The theoretical models and scenarios of the software package are described. Examples of application of the software package to solving the main problems arising in the design of magnetoresistive memory elements and consistent miniaturization of these devices are considered.

DOI: 10.1134/S1995078017020082

INTRODUCTION

Spintronics, as one of the most promising directions of the development of nano- and microelectronics, allows the use of magnetic degrees of freedom of localized and transport electrons for the creation of new functional microelectronic devices. The important milestones in the development of spintronics are the discovery of the giant magnetoresistive effect in 1988 [1] and of tunnel magnetoresistance (TMR) in 1996 [2]. These discoveries have been successfully used for the development of reading heads of hard drives with increased areal densities [3]. Magnetic random access memory devices (MRAM) provide another promising application of these discoveries. These devices ensure nonvolatile data storage with energy and read/write times comparable or exceeding those of semiconductor memory devices at an almost unlimited number of cycles, which makes them promising candidates for the development of universal nonvolatile memory [4]. These properties of MRAM devices ensure their successful application as memory modules in a broad range of electronic devices at the moment [5–7].

To develop new spintronic devices, one must have software tools for modeling the characteristics of such devices depending on the parameters of the device and the properties of magnetic materials. However, the existing software tools for the technology computer aided design (TCAD) simulation of microelectronic devices from such manufacturers as Synopsys [8], Silvaco [9], Cogenda [10], etc., do not include methods and models for calculating magnetization dynamics in spintronic devices. On the other hand, there is a set of packages for modeling of spintronic devices (MagOasis products companies [11], GoParallel [12], etc.), with universal 3D solvers of the micromagnetic problem, which cannot not calculate the distribution of thermal and mechanical fields, strongly affecting the performance of the spintronic device and its operation. Therefore, any product stated above has no complete functionality necessary for the TCAD simulation of spintronic devices based on the interaction of magnetic, thermal, and mechanical fields. The software package presented in this work significantly differs from the above ones, as it provides a possibility of carrying out multiphysical and multilevel calculations of spintronic devices. With this software package, one can optimize the parameters of spintronics nanodevices and study the possibility of the further miniaturization of these devices.

[1] The article is published in the original.

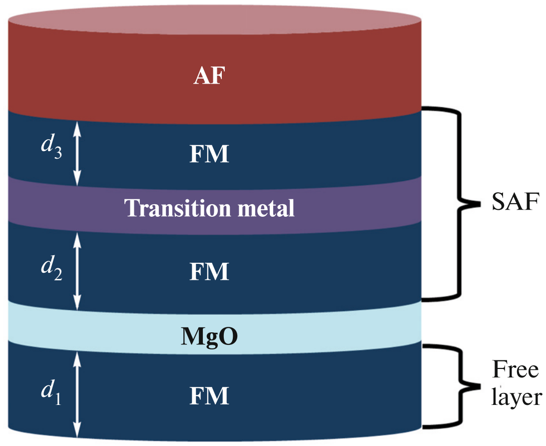

Fig. 1. (Color online) Schematic diagram of a FI TAS-MRAM memory unit.

BASIC DESIGNS OF SPINTRONIC DEVICES BASED ON MAGNETIC TUNNEL JUNCTIONS

The basic element of the considered spintronic devices is magnetic unit, which contains one magnetic tunnel junction (MTJ). MTJ is a multilayer nanostructure, in which two ferromagnetic (FM) layers are separated by a thin (~1 nm) insulating layer. The electrical conductivity of the MTJ is determined by the tunneling of electrons through the insulating layer. A key feature of the MTJ is the dependence of the electrical resistance of the mutual orientation of the magnetization of ferromagnetic layers. In particular, for the antiparallel orientation of magnetization vectors, resistance is higher than that for the parallel orientation. TMR is determined as the relative difference of resistances of antiparallel and parallel orientations of magnetization vectors. Recently, high TMR values exceeding 200% were obtained at room temperature for crystalline MgO tunnel barriers [13]. Thus, using tunnel magnetoresistance, one can rather precisely determine the state of magnetization in an MTJ and use it to read information. The direction of magnetization can be controlled by an external magnetic field in the ferromagnetic layers of MTJ (field induced, FI) or by the current through the magnetic tunnel junction because of the effect of spin-transfer torque (STT) [14]. Recently, alternative options of the control of magnetization state have also been studied based on the dependence of the vertical anisotropy of the magnetic thin layer on the voltage on the MTJ [15], on the effect of longitudinal spin-orbit spin switching [16], and on the magnetoelectric effect in multiferroic structures [17].

To ensure the stability of magnetization of the ferromagnetic layer, the energy barrier preventing its spontaneous switching due to thermal fluctuations must be sufficiently high. The barrier to switching magnetization is determined by magnetic anisotropy, which may be determined by the shape of functional layers (for example, elliptical shape is used to stabilize the orientation of magnetization along the major axis of the ellipse), magnetic anisotropy of a ferromagnetic material, or surface magnetic anisotropy at the interface between the layers. To increase the stability of magnetization in the ferromagnetic layers (data storage reliability), one should increase the magnetic anisotropy of the system; however, this inevitably increases the field and current thresholds to switching of magnetization in data recording.

To solve this problem, Åkerman et al. proposed a concept of thermally assisted switching (TAS), i.e., the reduction of energy barrier due to heating [18]. Today two methods of TAS implementation for overcoming the problem of scaling non-volatile magnetic components are known, namely, thermoassisted field record [19, 20] and thermoassisted spin-transfer torque [21, 22]. Thermal heating solves the problem of the reduction of the energy barrier in both cases.

The direction of magnetization of the free layer in the TAS-MRAM concept is fixed by exchange interaction at the “ferromagnetic/antiferromagnetic” interface, and thermal heating is used in the write process to increase temperature above the Neel temperature of the antiferromagnet to release the magnetization of the layer. Next, recording (magnetization switching) is made, and after cooling, the configuration is retained. Thus, the TAS-MRAM concept resolves the contradiction between the reliability of data storage and the efficiency of the switching process and opens a possibility of the further reduction of the size of MRAM devices [23].

The diagram of a current storage cell includes one MTJ element, connected to the bus and to a switching transistor, and one field line for generating magnetic field for MTJ switching. The thermal heating of an MTJ element is achieved by passing current through it, while lower currents are used to measure TMR values in the MTJ. The structure of an MTJ element of a MRAM unit is shown in Fig. 1. It includes a free (sensitive) ferromagnetic layer; a tunneling dielectric MgO layer; a synthetic antiferromagnet (SAF) consisting of two ferromagnetic layers separated by a thin layer of a transition metal; and an antiferromagnetic (AF) layer responsible for the fixing of the magnetization of the ferromagnetic layer closest to the SAF. The typical thickness of the ferromagnetic layers in an MTJ element is 2–3 nm, the thicknesses of the tunneling MgO and transition metal layers are about 1 nm or below. This MTJ structure is used for FI MRAM and STT-MRAM devices. In STT-MRAM devices, SAF is used as a reference layer for the creation of spin-polarized current.

Therefore, present-day MTJ-based spintronic devices are complex multilayer nanostructures, containing ferromagnetic and antiferromagnetic layers and based on the effect of exchange interaction

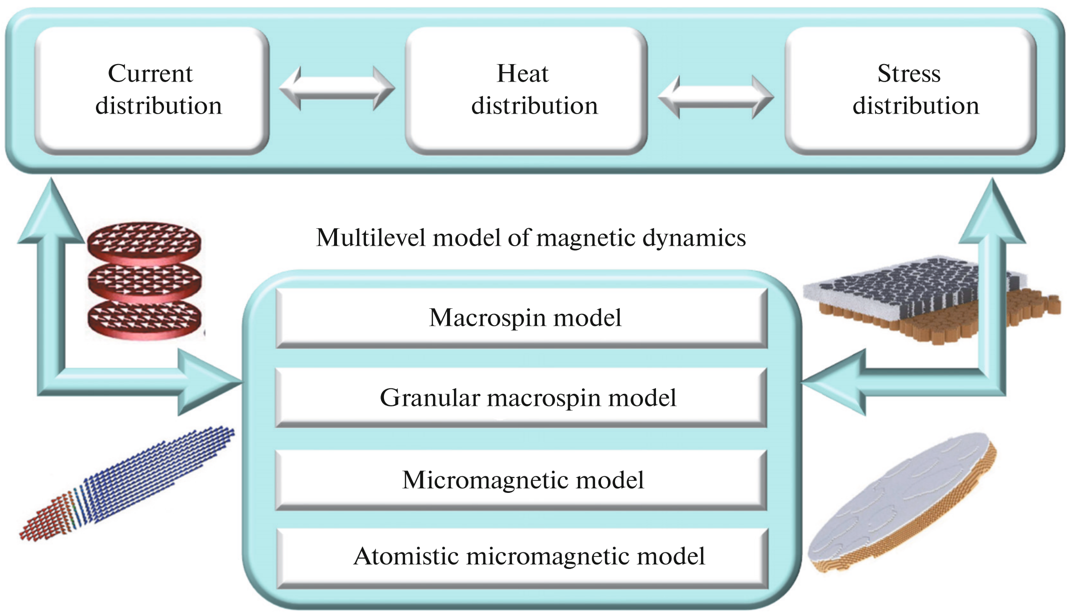

Fig. 2. (Color online) Multiphysical model of an MTJ-based spintronic nanodevice.

between the layers and processes of spin-transfer torque. In addition, spintronic devices with thermoassisted switching utilize Joule heating for the reversal of the magnetization of layers, which inevitably leads to the appearance of mechanical stress in the device. The presented software package allows the description of these effects and the simulation of magnetic dynamics and thermomechanics in spintronic nanostructures based on the mutual effect of the layers.

DESCRIPTION OF SOFTWARE PACKAGE

The software package for the device-technological modeling of MTJ-based spintronic nanodevices includes the following software components for the description of different physical properties of the devices.

1. A magnetic dynamics software component for the description of the evolution of magnetization in the layers of spintronic devices.

2. A software component for calculating the distribution of temperature, electric current, and mechanical stress in spintronic devices.

These software components can be used together to perform multiphysical calculations (see Fig. 2).

The magnetic dynamics software component is based on solving the Landau–Lifshitz–Gilbert equation for spin dynamics

$$\frac{\partial \mathbf{M}}{\partial t} = -\gamma[\mathbf{M}\times\mathbf{H}_{\mathrm{eff}}] - \gamma\frac{\alpha}{\mathrm{M_S}}\cdot[\mathbf{M}\times[\mathbf{M}\times\mathbf{H}_{\mathrm{eff}}]], \quad (1)$$

where $\mathbf{M}$ is magnetization vector at a given point, $\mathrm{M_S}$ is the saturation magnetization of the material, γ is electron gyromagnetic ratio, α is dimensionless damping parameter. This equation describes the evolution of magnetization $\mathbf{M}_i$ at each point i of the magnetic material in response to effective field $\mathbf{H}_{\mathrm{eff},i}$, including contributions from exchange interaction, magnetic anisotropy, applied external field $\mathbf{H}_{\mathrm{ext}}$, demagnetization field $\mathbf{H}_{\mathrm{d},i}$, spin-transfer torque $\mathbf{H}_{\mathrm{STT}}$, exchange bias field $\mathbf{H}_{\mathrm{EB}}$ at the interface, random field of thermal fluctuations $\mathbf{H}_{\mathrm{TN}}$, and magnetoelastic field $\mathbf{H}_{\mathrm{ME}}$:

$$\mathbf{H}_{\mathrm{eff},i} = \frac{2A}{\mathbf{M}_\mathrm{S}^2}\cdot\Delta\mathbf{M}_i(T) + \frac{2K(T)}{\mathbf{M}_\mathrm{S}^2}\cdot\mathbf{n}_i\cdot(\mathbf{n}_i\cdot\mathbf{M}_i) + \mathbf{H}_{\mathrm{d},i}(T) + \mathbf{H}_{\mathrm{ext}} + \mathbf{H}_{\mathrm{STT}} + \mathbf{H}_{\mathrm{EB}} + \mathbf{H}_{\mathrm{ME}} + \mathbf{H}_{\mathrm{TN}}, \quad (2)$$

where A is exchange coupling constant, K is anisotropy constant (taking into account dependence on temperature $(1 - T/T_\mathrm{c})$, where T_c is Curie temperature), $\mathbf{n}_i$ is magnetization easy axis. In addition, the Landau–Lifshitz–Bloch equation [24] can be used to take into account the temperature dependence of saturation magnetization. The Slonchevsky formalism [25] is used to describe spin-transfer torque.

The magnetic dynamics software component includes several models, implementing solutions of magnetic dynamics equation (1) with different levels of detailization.

The crudest model is the model of macrospin magnetic dynamics, in which the distribution of magnetization in the ferromagnetic layers of magnetic devices is supposed to be homogeneous. Within this description, the speed of integration of magnetic dynamics equations can be substantially increased, the behavior of the system under different impacts can be rapidly analyzed, and performance characteristics of devices, such as curves of magnetoresistance, etc., can be quickly calculated. The approach is widely used in the construction of phase diagrams of the reliability of spintronic devices, involving a great number of parametric calculations, and in the optimization of device parameters, e.g., geometry, by predetermined target functions.

The granular model of magnetic dynamics assumes uniform magnetization in each grain of a polycrystalline magnetic structure. Granular model implemented in a software package is designed for the simulation of spin dynamics in a heterostructure consisting of ferromagnetic and antiferromagnetic polycrystalline layers, taking into account the random thermal excitation of spins. The model can describe the process of temperature relaxation of a field of exchange bias in an exchange-coupled heterostructure with an ensemble of antiferromagnetic grains.

The standard micromagnetic model belongs to continuous medium models and ensures the description of smooth non-uniform distributions of magnetization in the space with variations noticeably exceeding atomic size. This model can describe magnetization distributions containing domain walls, vortices, etc.; however, it cannot directly describe antiferromagnetic and heteroatomic magnetic systems. For the description of such systems one should use model of atomistic magnetic dynamics, which is the most detailed model and considers each atom of the crystal lattice and the state of its intrinsic magnet moment. This approach ensures the account of the effects of non-uniform composition, defects in the material, roughness and complex shape boundaries, and also interactions of magnetic moments of different atoms for FM and AF materials.

In addition, the magnetic dynamics software component contains a module for calculating spin transport in tunnel junction with magnetic electrodes, which allows the calculation of TMR and spin torque moments transferred by conduction electrons in a tunnel spin-valve structure.

Thus, the presence of magnetic models with varied level of details allows the researcher to obtain solutions of magnetic dynamics equations in a wide range of spatial and time scales: from studying the effect of atomic structure on magnetic properties to the description of behavior at macroscopic times.

The software component for calculating thermal and electric fields and mechanical stresses in spintronic devices ensures the calculation of the static and dynamic distribution of these fields at the specified boundary conditions. The software component takes into account the dependence of the main physical properties of the material (thermal and electrical conductivity) on local temperature, TMR dependence on stress and temperature, and presence of residual stresses in different layers of the device and utilizes an elastoplastic model of material deformation.

A conjugation of the magnetic dynamics problem with the problem of the distribution of temperature, current, and mechanical stress is provided for building the multiphysical model. For this purpose, data exchange between the software components is executed and data are periodically synchronized between them. The software component for calculating temperature, voltage, and current distributions transfers these distributions to modules calculating magnetic dynamics, to describe magnetic properties of materials depending on temperature and spin transfer processes, as well as to take into account magnetoelastic interactions in ferromagnetic and antiferromagnetic layers. Modules calculating magnetic dynamics, in their turn, transfer calculated TMR values to the software component calculating temperature, current, and voltage distributions.

Integration of magnetic dynamics equations and equations of temperature, current, and mechanical stress distributions over time usually requires different time steps for a given accuracy of integration. Therefore, a process splitting method with the successive integration of equations for each component is used for the conjugation of both software components. As the integration step for magnetic dynamics is usually determined by the rate of magnetic precession and weakly depends on time (typical step is 10^{-13}–10^{-14} s), it is smaller than the typical time step for integrating equations of temperature, current, and mechanical stress distribution (typical step for this model is 10^{-11}–10^{-12} s). Therefore, in the software implementation of the process splitting method, the integration step of the heat problem was used as final time for the integration of magnetic dynamics equations.

The device structure is specified layer-by-layer using parametric extension of the GDS format [26]. Based on the layered structure of the device, the program generated a 3D structure of the device, which is recorded in the Netgen CSG format [27]. An example of a 3D structure of FI TAS MRAM spintronic devices with an array of four MTJ is shown in Fig. 3. Then, based on this 3D structure, the software generates a tetrahedral finite element mesh using the Netgen library [28]. The software component for calculating temperature, current, and mechanical stress distribution uses an irregular tetrahedral mesh. At the same time, the magnetic dynamics problem can be more conveniently solved on a regular rectangular mesh. As software components generally use different meshes, the software package includes mapping of these parameters between different grids of different software components and modules.

As a result of solving the problem, the researcher obtains files with the distribution of temperature, voltage, and mechanical stresses in the VTK format [29] for the 3D visualization of the results.

To analyze the sensitivity of the results to the parameters of the model, the software package allows parametric calculations; in addition, the code has an interface to the Dakota software package [30] for performing the analysis of sensitivity, propagation of uncertainties, and optimization.

To illustrate the application of the software package to TCAD modeling of MTJ-based spintronic nanodevices, let us consider the main problems arising in the design of such devices. In addition, based on the results obtained, we will analyze the main possibilities for the further miniaturization of spintronic devices.

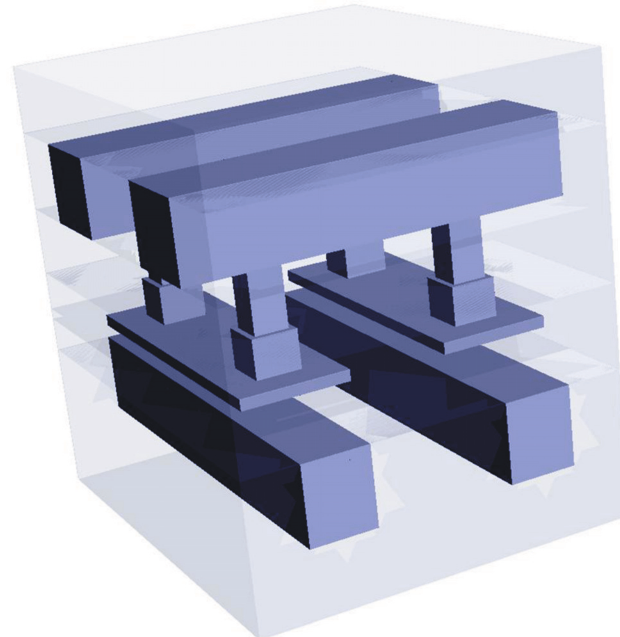

Fig. 3. (Color online) 3D model of a spintronic device with four magnetic tunnel junctions built from the structure defined in the GDS format.

CONSTRUCTION OF PHASE DIAGRAMS OF THE RELIABILITY OF THERMOASSISTED MAGNETIC MEMORY FIELD

In the field induced thermoassisted magnetic memory (FI TAS MRAM), the storage of information is attained in the direction of magnetization of the antiferromagnetic layer, which is used for the exchange fixing of ferromagnetic layers. A write operation in this case consists in heating the antiferromagnetic layer above the blocking temperature, at which exchange pinning of the ferromagnetic layer disappears. After heating, the applied magnetic field changes the orientation of the ferromagnetic layer adjacent to the antiferromagnetic layer. The magnitude of the generated magnetic field must be sufficient for overcoming the barriers of switching the magnetization of layers. To study fields required for successful writing in FI TAS MRAM devices, we performed calculations of the probability of switching magnetic layers, depending on the values of magnetic field and magnetic anisotropy of the ferromagnetic layers using the macrospin dynamics module. Calculations were performed for a three-layer structure with a synthetic uncompensated antiferromagnet with d_1 = 2.5 nm, d_2 = 2.0 nm, d_3 = 1.7 nm (see Fig. 1).

The calculated switching diagram is shown in Fig. 4a on the coordinates "value of magnetic anisotropy" vs. "external field" (K, $\mathbf{H}_{ext}$). For each point of the diagram, magnetic dynamics with the initial orientation of the magnetization of ferromagnetic layers in the horizontal plane with the angles $\phi_1 = 0°$, $\phi_2 = 180°$, and $\phi_3 = 0°$ relative to the direction of the external field was calculated. As can be seen in the figure, the diagram has three regions. The first region (left side of the diagram) corresponds to bipolar switching with all ferromagnetic layers rotated simultaneously; the second region (upper right part of the diagram) corresponds to switching of the free layer only (SAF layer does not rotate); and the third region at the bottom of the diagram corresponds to the complete absence of switching. It can be seen that, for small values of the magnetic anisotropy of ferromagnetic layers, there is a critical value of the external field at which switching is possible. However, for the coefficient of magnetic anisotropy higher than $K \geq 5K_0$, an increase in external field results in switching of only the free layer instead of bipolar switching, because the magnetostatic coupling between the free layer and SAF layers is not strong enough for overcoming magnetic anisotropy in the ferromagnetic layers. Thus, there occurs an upper limit for the coefficient of magnetic anisotropy of the ferromagnetic material for a successful write operation in devices of this type.

The phase diagram of switching for a read operation (change in the magnetization of the free layer; SAF layers are fixed by the antiferromagnetic layer) in FI TAS MRAM devices is shown in Fig. 4b. In this case, the diagram has only two regions, corresponding to switching of the free layer and to the absence of switching in the system. Switching of the free layer occurs when the external field exceeds a critical value, which increases with increasing magnetic anisotropy. Thus, the reduction of switching currents in FI TAS MRAM devices requires the reduction of the magnetic anisotropy of the material of the free layer.

DETERMINATION OF CRITICAL CURRENTS FOR MAGNETIC MEMORY WITH SWITCHING UNDER SPIN TRANSFER TORQUE

The key issue of switching magnetization under spin transfer torque in STT MRAM devices is a

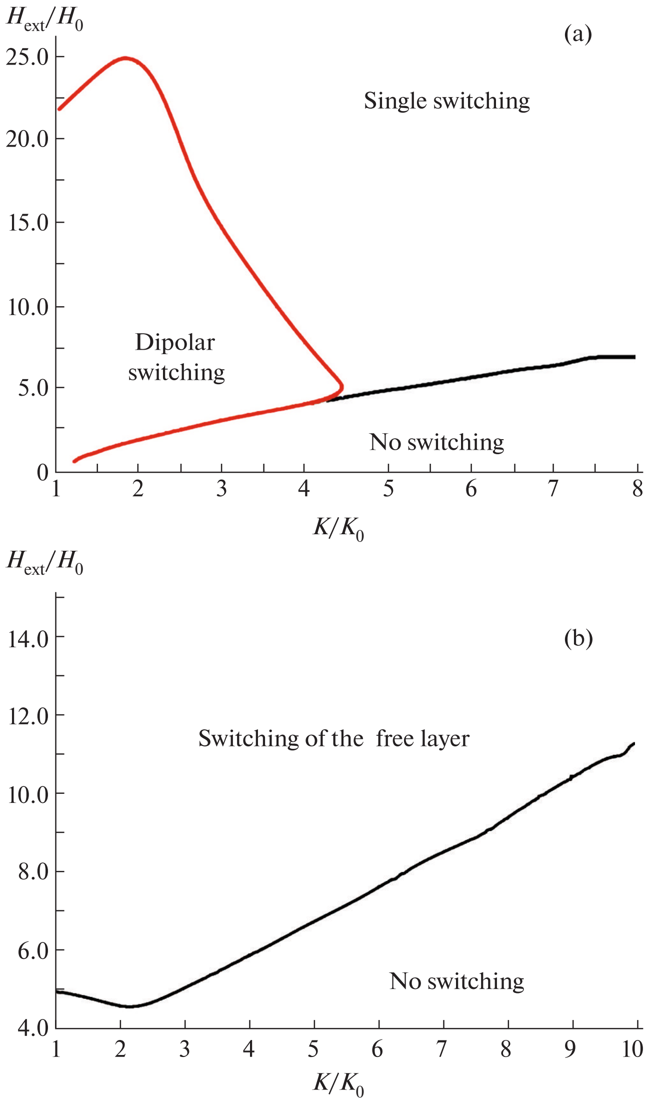

Fig. 4. (Color online) Regions of different types of switching in the MTJ element in FI TAS MRAM devices on the coordinates "anisotropy–magnetic field" calculated the using macrospin model: (a) write operation, (b) read operation.

decrease in critical current density, which is determined by the anisotropy and thickness of the free layer and the efficiency of spin polarization. The high density of critical current requires high voltages at the magnetic tunnel junction, which leads to the rapid degradation of the tunnel dielectric over time. Using the micromagnetic models, one can determine critical current values for a given geometry of the device and properties of magnetic materials. Using this model, calculations of switching probability due to spin transfer torque were performed for (1) parallel magnetization in an elliptic free layer of NiFe 80 nm in width and 160 nm in length, (2) perpendicular magnetization in a circular free layer of NiFe 80 nm in diameter with perpendicular magnetic anisotropy of $K = 5 \times 10^5$ J/m^3, depending on current density for different thicknesses of the free layer. Magnetization in the reference layer was fixed at an angle of 30° to the initial magnetization of the free layer, and the degree of spin polarization of current was 0.57. The initial magnetization in case (1) was directed along the major axis of the ellipse and, in case (2), perpendicularly to the layer. The results of calculations of the final magnetization of the free layer within 1 ns are shown in Fig. 5. It can be seen that critical switching current density decreases with decreasing thickness of the free layer and is of about 3×10^7 A/cm^2 for a thickness of 2.5 nm. Moreover, calculations show that the time of switching magnetization due to spin transfer torque strongly depends on the initial angle between the magnetizations of the free and reference layers, and, for their antiparallel orientation, switching is determined by thermal fluctuations of magnetization and results in non-deterministic switching behavior. It should be noted that the value of critical current density weakly depends on the diameter of the MTJ, which ensures the use of this method of switching magnetization for the subsequent miniaturization of spintronic nanodevices to a diameter of MTJ of 10 nm [31].

STUDY OF THE RELIABILITY OF DATA STORAGE IN STT MRAM MAGNETIC MEMORY DEVICES

The safety of the written information is one of the key parameters of memory devices. As was estimated in [18], for storage within 10 years, the energy barrier for switching must exceed $65k_BT$, where T is temperature and k_B is Boltzmann constant, for thermal fluctuations could not lead to spontaneous switching. For nanosized magnetic memory devices, switching is usually due to a uniform rotation of magnetization (Stoner–Wohlfarth mechanism [32]). In this case, the energy barrier to switching is determined by the product K_uV, where K_u is magnetic anisotropy constant (usually it is shape anisotropy of the free layer) and V is volume of the magnetic element. Therefore, to increase the barrier, magnetic anisotropy can be increased by increasing aspect ratio of the free layer for spintronic devices with longitudinal magnetization, or by increasing the volume of the magnetic element. However, above a certain critical threshold, switching of magnetization in MRAM devices can occur through the propagation of the domain wall rather than through the uniform rotation of magnetization. To determine the critical threshold value, we calculated the energy barrier for both switching mechanisms for an elliptic free layer 80 nm in width and 2.5 nm in thickness with aspect ratio of 1.5–3.2. This was done using the Nudged Elastic Band (NEB) method [33], which ensures the calculation of switching path for the given initial and final states of the system and is implemented in the micromagnetic dynamics module. The results of calculations of switching

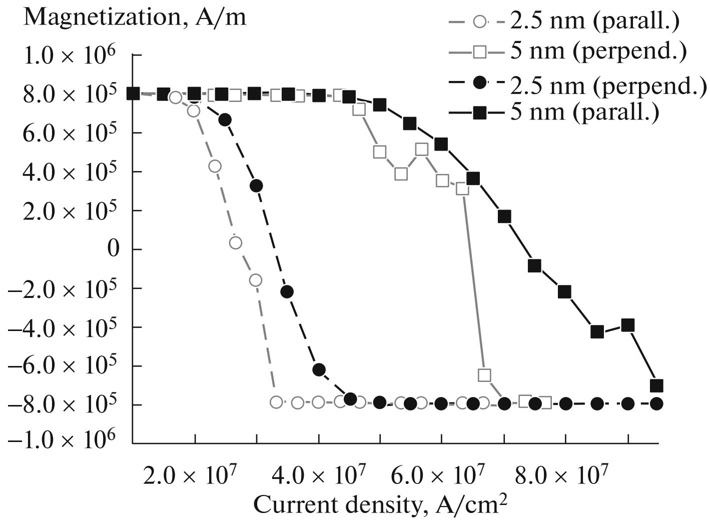

Fig. 5. Dependence of the final magnetization of the free layer (projection of the initial magnetization direction) within 1 ns for switching STT MRAM on current density for different thicknesses of the recording layer.

barriers are shown in Fig. 6. It can be seen that, for the aspect ratio >2.2, the barrier to uniform rotation exceeds the barrier to the propagation of the domain wall and the barrier slightly changes at a further increase in the aspect ratio. Therefore, the stability of data storage in MRAM devices is not improved at a further increase in the aspect ratio of the free layer. MRAM devices with perpendicular magnetization offer the best potential to scaling, because they do not require the use of MTJ of elliptical shape. To ensure the stability of data storage in the subsequent miniaturization of spintronic nanodevices, one can use the thermoassisted switching method (STT TAS MRAM) discussed above, in which data are stored in the magnetization of the antiferromagnetic layer.

DETERMINATION OF CRITICAL CURRENTS FOR SWITCHING THE THERMOASSISTED MAGNETIC MEMORY

As was mentioned above, the write operation in a FI TAS MRAM device is carried out by passing an electric current through the MTJ element. The antiferromagnetic layer is heated above the blocking temperature and the demagnetization of the free layer occurs, because of which a write operation is performed.

The structure considered in this example and shown in Fig. 3 is an array of four MTJ, connected by two straps and two upper lines, and also including two field lines. The array of MTJ and the supply lines are encapsulated into a silica matrix. Critical current was determined using the software component for calculating temperature, electric current, and mechanical stress distributions in spintronic devices.

An example of a calculated temperature distribution in an MTJ is shown in Fig. 7. It can be seen in the figure that temperature is increased only in the magnetic tunnel junction, where heat is generated in the MgO layer. Outside the layer, temperature decreases in the neighboring layers, and far from the MTJ, temperature virtually coincides with the room temperature. Therefore, a small power of Joule heating may be required to rewrite the element. In fact, calculations showed that, to achieve blocking temperature of the antiferromagnetic layer equal to 500 K in the MTJ, current density must be of about 4 MA/cm^2, which is significantly lower than current density required to

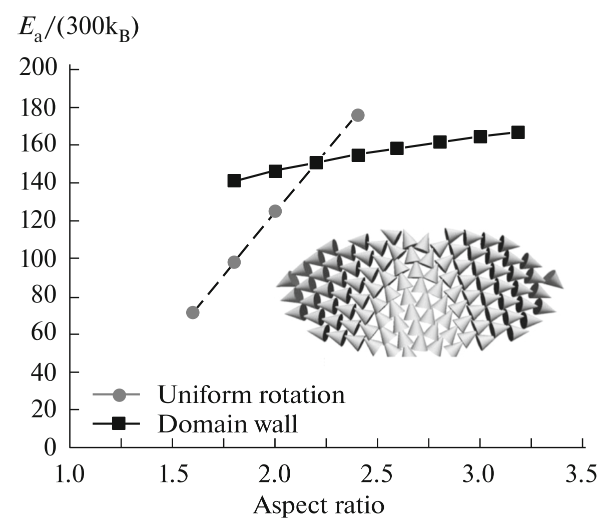

Fig. 6. Dependence of energy barrier to switching STT MRAM for mechanisms of uniform rotation and propagation of the domain wall (see inset) on the aspect ratio of the STT MRAM free layer.

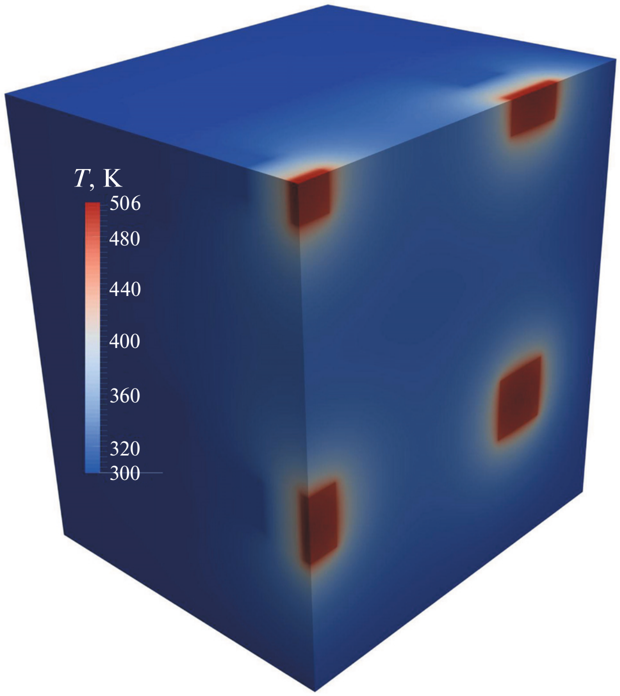

Fig. 7. (Color online) Calculated temperature distribution in the write operation (the structure is cut by three planes passing through the center of one MTJ).

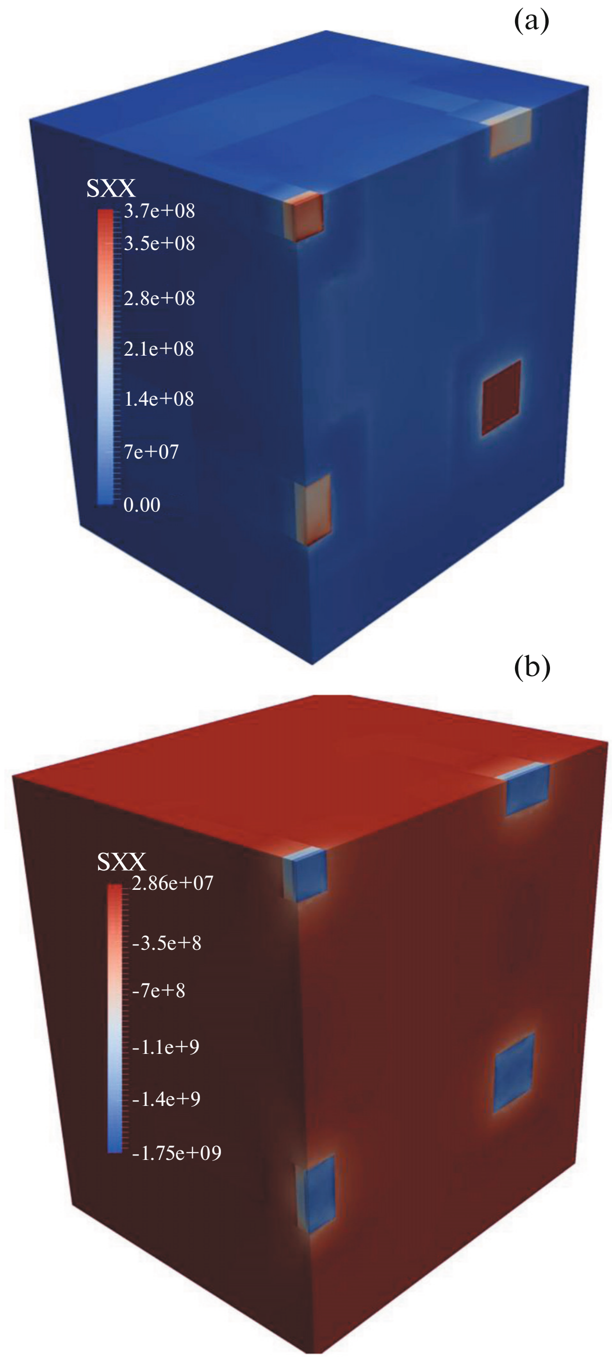

Fig. 8. (Color online) Calculated distribution of the σ_{xx} stress component in (a) read and (b) write operations (the structure is cut by three planes passing through the center of one MTJ).

switch STT MRAM (see Fig. 5). Note that the method of thermoassisted switching ensures the possibility of scaling down spintronic devices to a technology of 20 nm [34], because heating current density weakly depends on MTJ size.

Let us additionally note that, because of the low value of thermal conductivity of the strap material and dielectric matrix, a strong and non-uniform heating of these layers occurs, which causes mechanical stresses in them because of a difference in the thermal expansion coefficients of the materials. These stresses are, in turn, transmitted to MTJ ferromagnetic layers. Consequently, it can be expected that the values of mechanical stresses in MTJ strongly vary during the read (in the absence of heating) and write operations. In fact, on an example of the σ_{xx} stress component shown in Fig. 8, one can see that mechanical stresses during the read operation are close to zero, while for write operation, they can reach 1.7 GPa for the given geometry. Mechanical stresses in MTJ ferromagnetic layers can significantly affect magnetic properties, in particular, the value of tunnel magnetoresistance [35].

INVESTIGATION OF FIELD LINE GENERATION EFFICIENCY IN FI MRAM DEVICES

To change the state of a spintronic device with field-induced switching of FI MRAM, one should apply an external magnetic field. For this purpose, special lines, called field lines, are used, which create a magnetic field in a magnetic tunnel junction under the influence of a current pulse. However, current density in the field line required for switching of the state of a spintronic device increases with a decrease in

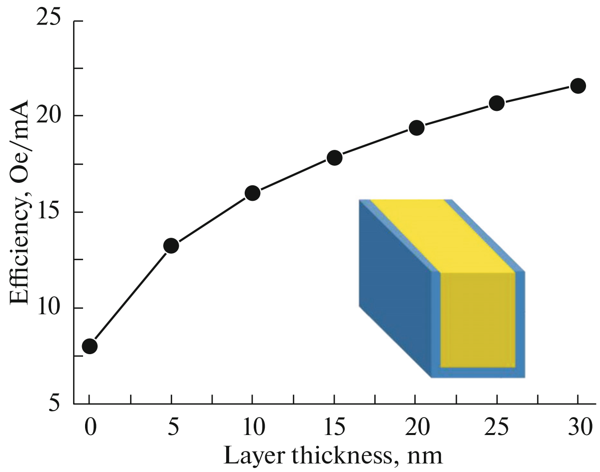

Fig. 9. (Color online) Calculated dependence of field line generation efficiency on the thickness of ferromagnetic layer for the current 10 mA. The inset shows the ferromagnetic shield of the field line.

the size of field line, which creates difficulties in the miniaturizing of devices. To overcome this problem, it was proposed to use ferromagnetic shields, ensuring the concentration of magnetic field in the MTJ region. In scaling spintronic devices, there also arises a question about the efficiency of the shielding properties of nanoscale ferromagnetic layers. The efficiency of the shielding properties of the ferromagnetic coating around the field line is usually characterized by the ratio of the generated magnetic field at a specified point to the value of current in the field line (so-called "field generation efficiency").

The micromagnetic model was used to simulate shielding effects in nanoscale ferromagnetic screens. A copper field line 200 nm in width and 300 nm in height with a ferromagnetic NiFe coating (see inset in Fig. 9) was considered. The dependence of field generation efficiency on the thickness of the ferromagnetic layer is shown in Fig. 9. It can be seen that the efficiency of the field line was increased two- to threefold compared to that of the field line without a coating, and for very thin coatings (smaller than 10 nm for the given line geometry), the generated field significantly degraded because of the achievement of the saturation of magnetization of the ferromagnetic layer [36].

Therefore, despite the fact that the use of ferromagnetic shields ensures a significant increase in the efficiency of field generation, there are restrictions on scalability for MTJ diameters smaller than 45 nm, associated with a decrease in the efficiency of magnetic shielding in ferromagnetic nanolayers and the need in increasing current density.

CONCLUSIONS

In this paper, we described software for the TCAD modeling of spintronics nanodevices based on magnetic tunnel junctions. The software includes a multilevel multiphysical model for describing magnetic dynamics and for calculating temperature, electric current, and mechanical stress distributions, ensuring the simulation of magnetic dynamics and thermomechanics in spintronic nanodevices taking into account the mutual influence of layers. Examples of application of the software package to solving the main problems in the design and miniaturization of spintronics nanodevices, such as the determination of the critical parameters for switching magnetization, and also to the estimation of the stability of the data stored in the magnetic form. It is noted that spintronic devices based on field induced magnetization switching have scalability limitations for sizes smaller than 45 nm, associated with a decrease in the efficiency of magnetic shielding in ferromagnetic nanolayers and the need in increasing current density. Spintronic devices based on spin transfer torque may be scaled down to 10 nm, because current density for switching weakly depends on the size of magnetic tunnel junction. The problem of the stability of storage of magnetic information in scaling spintronic devices can be solved using thermoassisted switching. However, it is necessary to consider that thermoassisted switching leads to significant mechanical stresses in heating the magnetic tunnel junction, which may affect switching thresholds.

ACKNOWLEDGMENTS

The work was supported by the Ministry of Education and Science of the Russian Federation (contract RFMEFI57614X0023).

REFERENCES

1. M. N. Baibich, J. M. Broto, A. Fert, et al., "Giant magnetoresistance of (001)Fe/(001)Cr magnetic superlattices," Phys. Rev. Lett. **61**, 2472–2475 (1988).
2. J. S. Moodera, L. R. Kinder, T. M. Wong, et al., "Large magnetoresistance at room temperature in ferromagnetic thin film tunnel junctions," Phys. Rev. Lett. **74**, 3273–3276 (1995).
3. J. J. M. Ruigrok, R. Coehoorn, S. R. Cumpson, et al., "Disk recording beyond 100 Gb/in.2: Hybrid recording?," J. Appl. Phys. **87**, 5398–5403 (2000).
4. J. Åkerman, "Toward a universal memory," Science **308**, 508–510 (2005).
5. A. F. Popkov, K. A. Zvezdin, M. Yu. Chinenkov, et al., "Spin transport and problems of magnetic random access memory (MRAM)," Inzh. Fiz., No. 9, 19–34 (2012).
6. Y. Chen, H. H. Li, X. Wang, et al., "A 130 nm 1.2/3.3 V 16 kb spin-transfer torque random access memory with nondestructive self-reference sensing scheme," IEEE J. Solid-State Circuits **47**, 560–573 (2012).

7. B. Dieny, R. Sousa, S. Bandiera, et al., "Extended scalability and functionalities of MRAM based on thermally assisted writing," in *Proceedings of the Electron Devices Meeting IEDM* (IEEE Int., 2011), pp. 1.3.1–1.3.4.
8. www.synopsys.com. Accessed September 29, 2016.
9. www.silvaco.com. Accessed September 29, 2016.
10. www.cogenda.com. Accessed September 29, 2016.
11. www.magoasis.com. Accessed September 29, 2016.
12. www.goparallel.net. Accessed September 29, 2016.
13. S. S. P. Parkin, C. Kaiser, A. Panchula, et al., "Giant tunnelling magnetoresistance at room temperature with MgO (100) tunnel barriers," Nat. Mater. **3**, 862–867 (2004).
14. Y. Huai, "Spin-transfer torque MRAM (STT-MRAM): challenges and prospects," AAPPS Bull. **18**, 33–40 (2008).
15. M. Miron, K. Garello, G. Gaudin, et al., "Perpendicular switching of a single ferromagnetic layer induced by in-plane current injection," Nature **476**, 189–193 (2011).
16. Y.-W. Yin, M. Raju, W.-J. Hu, et al., "Multiferroic tunnel junctions," Front. Phys. **7**, 380–385 (2012).
17. T. Mauyama, Y. Shiota, T. Nozaki, et al., "Large voltage-induced magnetic anisotropy change in a few atomic layers of iron," Nat. Nanotechnol. **4**, 158–161 (2009).
18. J. Åkerman, M. DeHerrera, M. Durlam, et al., in *Magnetic Tunnel Junction Based Magnetoresistive Random Access Memory,* Ed. by M. Johnson (Elsevier Academic, Amsterdam, 2004).
19. J. Deak, "Thermal magnetic random access memory," in *Proceedings of the IEEE International Conference on Computer Design New Memory Technologies, San Jose, CA, Oct. 4, 2005.*
20. B. Purnama, Y. Nozaki, and K. Matsuyama, "Micromagnetic simulation of thermally assisted magnetization reversal in magnetic nanodots with perpendicular anisotropy," J. Magn. Magn. Mater. **310**, 2683–2685 (2007).
21. D. Pinna, A. Mitra, D. L. Stein, et al., "Thermally assisted spin-transfer torque magnetization reversal in uniaxial nanomagnets," Appl. Phys. Lett. **101**, 262401 (2012).
22. W. H. Butler, T. Mewes, C. K. A. Mewes, et al., "Switching distributions for perpendicular spin-torque devices within the macrospin approximation," IEEE Trans. Magn. **48**, 4684–4700 (2012).
23. I. L. Prejbeanu, S. Bandiera, J. Alvarez-Herault, et al., "Thermally assisted MRAMs: ultimate scalability and logic functionalities," J. Phys. D: Appl. Phys. **46**, 074002 (2013).
24. D. A. Garanin, "Fokker-Planck and Landau-Lifshitz-Bloch equations for classical ferromagnets," Phys. Rev. B **55**, 3050 (1997).
25. J. Slonczewski, "Current-driven excitation of magnetic multilayers," J. Magn. Magn. Mater. **159**, L1 (1996).
26. http://www.bitsavers.org/pdf/calma/GDS_II_Users_Operating_Manual_Nov78.pdf. Accessed November 30, 2016.
27. https://sourceforge.net/projects/netgen-mesher. Accessed September 29, 2016.
28. https://gitlab.asc.tuwien.ac.at/jschoeberl/ngsolve-docu/wikis/home. Accessed September 29, 2016.
29. http://www.vtk.org. Accessed September 29, 2016.
30. http://dakota.sandia.gov. Accessed November 30, 2016.
31. J. J. Nowak, R. P. Robertazzi, J. Z. Sun, et al., "Dependence of voltage and size on write error rates in spin-transfer torque magnetic random-access memory," IEEE Magn. Lett. **7**, 3102604 (2016).
32. E. C. Stoner and E. P. Wohlfarth, "A mechanism of magnetic hysteresis in heterogeneous alloys," Philos. Trans. R. Soc. London, Ser. A **240**, 599–642 (1948).
33. P. F. Bessarab, V. M. Uzdin, and H. Jonsson, "Method for finding mechanism and activation energy of magnetic transitions, applied to skyrmion and antivortex annihilation," Comput. Phys. Commun. **196**, 335–347 (2015).
34. I. L. Prejbeanu, S. Bandiera, J. Alvarez-Herault, et al., "Thermally assisted MRAMs: ultimate scalability and logic functionalities," J. Phys. D: Appl. Phys. **46**, 074002 (2013).
35. L. M. Loong, X. Qiu, Zh. P. Neo, et al., "Strain-enhanced tunneling magnetoresistance in MgO magnetic tunnel junctions," Sci. Rep. **4**, 6505 (2014).
36. I. M. Iskandarova, A. A. Knizhnik, A. F. Popkov, et al., "Micromagnetic modeling of the shielding properties of nanoscale ferromagnetic layers," J. Appl. Phys. **120**, 123903 (2016).